



HAL
open science

Dynamics of coupled Dahl type and non-smooth systems at different scales of time

Alireza Ture Savadkoohi, Claude-Henri Lamarque

► **To cite this version:**

Alireza Ture Savadkoohi, Claude-Henri Lamarque. Dynamics of coupled Dahl type and non-smooth systems at different scales of time. *International journal of bifurcation and chaos in applied sciences and engineering* , 2013, 23 (7), pp.1350114. 10.1142/S0218127413501149 . hal-00838822

HAL Id: hal-00838822

<https://hal.science/hal-00838822>

Submitted on 25 May 2024

HAL is a multi-disciplinary open access archive for the deposit and dissemination of scientific research documents, whether they are published or not. The documents may come from teaching and research institutions in France or abroad, or from public or private research centers.

L'archive ouverte pluridisciplinaire **HAL**, est destinée au dépôt et à la diffusion de documents scientifiques de niveau recherche, publiés ou non, émanant des établissements d'enseignement et de recherche français ou étrangers, des laboratoires publics ou privés.

Dynamics of coupled Dahl type and nonsmooth systems at different scales of time

A.TURESAVADKOOHI* and C.-H. LAMARQUE†
*Université de Lyon, ENTPE, LGCB and LTDS UMR CNRS 5513,
3 rue Maurice Audin, Vaulx-en-Velin Cedex, F-69518, France*

**alireza.turesavadkoohi@entpe.fr
†lamarque@entpe.fr*

Vibratory behavior of two coupled oscillators is studied. The main system — Dahl type — is coupled to a very light system with a nonsmooth potential that can be endowed for passively controlling the main system. Invariant manifold of the system at the fast time scale is revealed and the system behavior at slow time scale around the infinity of the fast time scale is detected. This can give us the chance to forecast all possible attractors of the system during energy exchange between the two oscillators.

Keywords: Bouc–Wen; Dahl; nonsmooth; energy pumping; control; bifurcation.

1. Introduction

Cubic nonlinear innate of some light oscillators namely, nonlinear energy sink devices (NES), has been proved to be a good choice for passive control and absorbing high amount of vibratory energy of linear important systems [Vakakis, 2001; Gendelman *et al.*, 2001; Vakakis & Gendelman, 2001; Gendelman, 2004; Gendelman & Lamarque, 2005; Gendelman *et al.*, 2006; Manevitch *et al.*, 2007a; Manevitch *et al.*, 2007b; Manevitch *et al.*, 2007c; Vakakis *et al.*, 2009a, 2009b; Starosvetsky & Gendelman, 2009, 2010; Gendelman *et al.*, 2011; Vigié & Kerschen, 2010; Manevitch *et al.*, 2011; Pham *et al.*, 2010, 2011a; Pham *et al.*, 2011b; Pham *et al.*, 2012; Vaurigaud *et al.*, 2011a; Vaurigaud *et al.*, 2011b, 2011c; Ture Savadkoochi *et al.*, 2011a]. These systems are verified experimentally as well [McFarland *et al.*, 2005a; McFarland *et al.*, 2005b; Kerschen *et al.*, 2007a; Kerschen *et al.*, 2007b; Gourdon *et al.*, 2007a; Gourdon *et al.*, 2007b; Lee *et al.*, 2007; Lee *et al.*, 2008; Lee *et al.*, 2010; Ture Savadkoochi *et al.*, 2012a].

There have been some attempts to consider other kinds of NES devices or main systems during recent years. Nucera *et al.* [2007] and Lee *et al.* [2009] studied energy pumping in systems with vibro-impact NES, while the energy pumping in a 2-dof system consisting of a linear dof and a nonlinear energy sink with nonpolynomial and piecewise potential was investigated by Gendelman [2008]. Schmidt and Lamarque [2010] studied the energy transfer from initial single dof system including nonsmooth term of friction to a NES under free transient or periodic external solicitations. Lamarque *et al.* [2011] analyzed the targeted energy transfer phenomenon from a linear master dof system to a Nonsmooth NES (NSNES) under different forcing conditions. They did a detailed investigation on the strongly modulated response (SMR) of the system and necessary conditions for its existence. Recently, Lamarque *et al.* [2012] analyzed multiscales dynamics of a nonsmooth main system and a NSNES. They revealed different invariants of the system at different infinities of time layers

with detecting stability zones of the system at each time layer. They showed that the system may get attracted to different fixed points at different scales of time which should be considered very carefully in the control process. Real behavior of some systems not only depends on their current state but also on their past states, which is called hysteresis behavior. For instance, hysteresis response of some of the structural elements (e.g. semi-rigid joints of a structure) during an earthquake or cyclic loadings [Ture Savadkoohi *et al.*, 2011b] and hysteresis behavior of magnetorheological/ electrorheological fluid dampers and shape-memory alloys [Awrejcewicz *et al.*, 2008]. So, for detecting or identifying the real behavior of systems, an appropriate hysteresis model should be used. The so-called Bouc–Wen class of hysteresis models in functional form was originally proposed by Bouc [1967, 1971] and generalized by Wen [1976]. Meanwhile, Dahl [1968] proposed a model which was an alternative to the Coulomb model for dry friction [Ikhouane & Rodellar, 2007]. Bouc–Wen class of hysteresis is widely used [Song & Der Kiureghian, 2006] due to their simplicity in analytical and computational treatments, since only one auxiliary nonlinear equation describes the hysteretic behavior, their application in nonlinear random vibration and their ability in describing various characteristics of hysteretic behavior such as degradation of stiffness and strength, pinching effect, biaxial hysteresis and asymmetry of the peak restoring force. However, an important drawback of Bouc–Wen type hysteresis models is local violation of plasticity theory where they may produce negative energy dissipation during unloading/reloading process without load reversal [Casciati, 1987; Thyagarajan & Iwan, 1990]. Nevertheless, they facilitate deterministic and stochastic dynamic analysis of real systems in the field of mechanical and structural engineering with reasonable and acceptable accuracy [Song & Der Kiureghian, 2006].

In this paper, we try to understand multiscale dynamics of two coupled nonsmooth oscillators, where the main one is Bouc–Wen type in general and Dahl type in particular and the other one is a simple nonsmooth oscillator which is attached to the main oscillator for the sake of control or energy harvesting. The organization of the paper is as follows: Governing equations of the system and their rescaled and averaged forms are developed in Sec. 2. The behavior of the system at the fast time scale is

emphasized in Sec. 3 while its behavior at the slow time scale in general and around its behavior at the fast time scale in particular, with some information on the stability analysis is studied in Sec. 4. Some numerical examples are collected in detail in Sec. 5. Finally, the paper is concluded in Sec. 6.

2. Governing Equations of the System and Their Averaged Forms

Let us consider a Bouc–Wen type main system [Song & Der Kiureghian, 2006] with the mass M under external forcing term $\tilde{f}(t) = \Gamma \sin(\Omega t)$ that is coupled to a NSNES with mass m , where $0 < \epsilon = \frac{m}{M} \ll 1$. The mathematical model of this system at the time domain t can be summarized as follows:

$$\begin{cases} M\ddot{x}_1 + C\dot{x}_1 + aK_1x_1 + (1-a)K_1x_3 \\ \quad + \tilde{F}(x_1 - x_2) + \tilde{\lambda}(\dot{x}_1 - \dot{x}_2) = \Gamma \sin(\Omega t) \\ m\ddot{x}_2 + \tilde{\lambda}(\dot{x}_2 - \dot{x}_1) + \tilde{F}(x_2 - x_1) = 0 \\ \dot{x}_3 = A\dot{x}_1 - \beta|\dot{x}_1||x_3|^{n-1}x_3 - \gamma\dot{x}_1|x_3|^n \end{cases} \quad (1)$$

where $x_3(0) = 0$ and $A, \beta > 0, \gamma$ and n are dimensionless quantities controlling the behavior of the model. \tilde{F} is the nonsmooth potential function of the NSNES which is defined as follows:

$$\begin{aligned} \tilde{F}(\alpha) &= -\frac{\partial V(\alpha)}{\partial \alpha} = -\tilde{F}(-\alpha) \\ &= \begin{cases} 0 & \text{if } -\delta \leq \alpha \leq \delta \\ K_2(\alpha - \delta) & \text{if } \alpha \geq \delta \\ K_2(\alpha + \delta) & \text{if } \alpha \leq -\delta. \end{cases} \end{aligned} \quad (2)$$

Let us shift the system to time scale $T = t\sqrt{\frac{ak_1}{M}} = t\vartheta$. The system (1) reads $(x_j(t) \mapsto y_j(T), j = 1, 2$ and $x_3(t) \mapsto z(T))$:

$$\begin{cases} \ddot{y}_1 + \epsilon\zeta\dot{y}_1 + y_1 + \frac{1-a}{a}z + \epsilon\hat{F}(y_1 - y_2) \\ \quad + \epsilon\lambda(\dot{y}_1 - \dot{y}_2) = \epsilon f_0 \sin(\omega T) \\ \epsilon\ddot{y}_2 + \epsilon\hat{F}(y_2 - y_1) + \epsilon\lambda(\dot{y}_2 - \dot{y}_1) = 0 \\ \dot{z} = Ay_1 - \beta|\dot{y}_1||z|^{n-1}z - \gamma\dot{y}_1|z|^n \end{cases} \quad (3)$$

where $\epsilon\zeta = \frac{C}{\sqrt{aK_1M}}$, $\epsilon\lambda = \frac{\tilde{\lambda}}{\sqrt{aK_1M}}$, $\frac{1}{aK_1}\tilde{F}(\alpha) = \epsilon\hat{F}(\alpha)$, $k = \frac{1}{\epsilon}\frac{K_2}{aK_1}$, $\omega = \frac{\Omega}{\vartheta}$ and $\frac{\Gamma}{aK_1} = \epsilon f_0$. The scaled

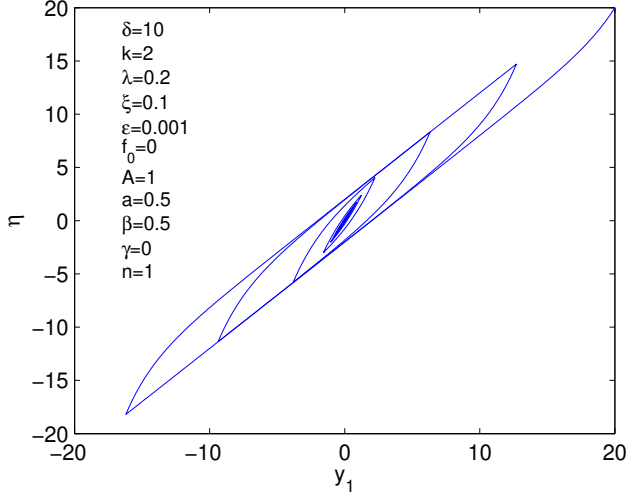


Fig. 1. y_1 versus η .

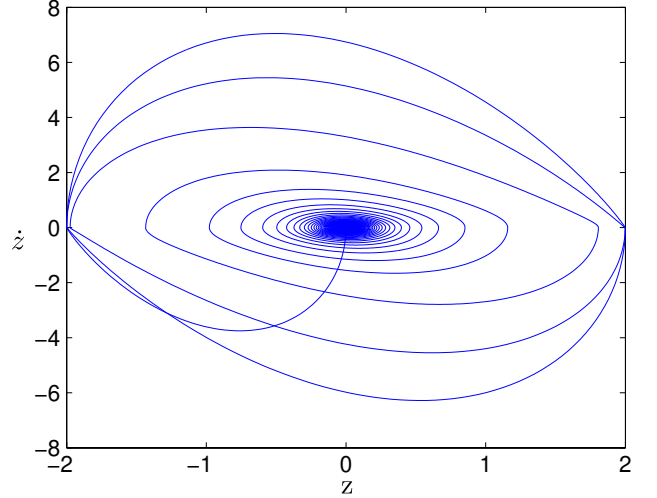


Fig. 2. z versus \dot{z} .

system potential of the NSNES reads as:

$$\hat{F}(\alpha) = \begin{cases} 0 & \text{if } -\delta \leq \alpha \leq \delta \\ k(\alpha - \delta) & \text{if } \alpha \geq \delta \\ k(\alpha + \delta) & \text{if } \alpha \leq -\delta. \end{cases} \quad (4)$$

The Dahl model [Ikhouane & Rodellar, 2007] of the mentioned system which is the aim of this paper can be obtained by setting $n = 1$ and $\gamma = 0$. Typical behaviors of these kinds of systems for some given parameters are depicted in Figs. 1 and 2, where

$$\eta = \epsilon \zeta \dot{y}_1 + y_1 + \frac{1-a}{a} z + \epsilon \hat{F}(y_1 - y_2) + \epsilon \lambda (\dot{y}_1 - \dot{y}_2). \quad (5)$$

These results are obtained by direct integration of Eq. (3) with the “ode45” function of Matlab. The following initial conditions have been chosen for the system:

$$\begin{cases} y_1(0) = 20, & \dot{y}_1(0) = 0 \\ y_2(0) = 0, & \dot{y}_2(0) = 0 \end{cases} \quad (6)$$

It should be mentioned that if $a = 1$, then the effect of Dahl model will disappear and the main system will remain linear. We are interested to analyze system (3) in the vicinity of 1:1 resonance. Let us transfer it to the following coordinates:

$$\begin{cases} v = y_1 + \epsilon y_2 \\ w = y_1 - y_2 \end{cases} \quad (7)$$

we have,

$$\begin{cases} \ddot{v} + \frac{\epsilon \zeta}{1+\epsilon} (\dot{v} + \epsilon \dot{w}) + \frac{1}{1+\epsilon} (v + \epsilon w) + \frac{1-a}{a} z = \epsilon f_0 \sin(\omega T) \\ \ddot{w} + \frac{\epsilon \zeta}{1+\epsilon} (\dot{v} + \epsilon \dot{w}) + \frac{1}{1+\epsilon} (v + \epsilon w) + \frac{1-a}{a} z + (1+\epsilon) \hat{F}(w) + (1+\epsilon) \lambda \dot{w} = \epsilon f_0 \sin(\omega T) \\ \dot{z} = A \frac{\dot{v} + \epsilon \dot{w}}{1+\epsilon} - \beta \left| \frac{\dot{v} + \epsilon \dot{w}}{1+\epsilon} \right| |z|^{n-1} z - \gamma \frac{\dot{v} + \epsilon \dot{w}}{1+\epsilon} |z|^n. \end{cases} \quad (8)$$

Complex variables of Manevitch [2001] are applied to the system as follows:

$$\begin{cases} \varphi_1 e^{i\omega T} = \dot{v} + i\omega v \\ \varphi_2 e^{i\omega T} = \dot{w} + i\omega w \\ \varphi_3 e^{i\omega T} = \dot{z} + i\omega z \end{cases} \quad (9)$$

where $i = \sqrt{-1}$. The averaged form of the system (8) in the vicinity of 1:1 resonance i.e. $\omega = 1 + \sigma\epsilon$ reads:

$$\left\{ \begin{array}{l} \dot{\varphi}_1 + \frac{i}{2}(1 + \sigma\epsilon)\varphi_1 + \frac{\epsilon\zeta}{2(1 + \epsilon)}(\varphi_1 + \epsilon\varphi_2) - \frac{i}{2(1 + \epsilon)(1 + \sigma\epsilon)}(\varphi_1 + \epsilon\varphi_2) - \frac{1 - a}{a} \frac{i}{2(1 + \sigma\epsilon)}\varphi_3 = \frac{\epsilon f_0}{2i} \\ \dot{\varphi}_2 + \frac{i}{2}(1 + \sigma\epsilon)\varphi_2 + \frac{\epsilon\zeta}{2(1 + \epsilon)}(\varphi_1 + \epsilon\varphi_2) - \frac{i}{2(1 + \epsilon)(1 + \sigma\epsilon)}(\varphi_1 + \epsilon\varphi_2) - \frac{1 - a}{a} \frac{i}{2(1 + \sigma\epsilon)}\varphi_3 \\ \quad - \frac{i}{2}(1 + \epsilon)\varphi_2 G(|\varphi_2|^2) + \frac{1 + \epsilon}{2}\lambda\varphi_2 = \frac{\epsilon f_0}{2i} \\ \varphi_3 = \frac{A}{1 + \epsilon}(\varphi_1 + \epsilon\varphi_2) + \frac{i\beta e^{-i\delta_1(1 + \sigma\epsilon)}}{12\pi(1 + \epsilon)(1 + \sigma\epsilon)}(3(\varphi_1 + \epsilon\varphi_2)\varphi_3 + e^{4i\delta_1(1 + \sigma\epsilon)}(\varphi_1^* + \epsilon\varphi_2^*)\varphi_3^* \\ \quad + 3e^{2i\delta_1(1 + \sigma\epsilon)}(\varphi_1^*\varphi_3 + \epsilon\varphi_2^*\varphi_3 - \varphi_1\varphi_3^* - \epsilon\varphi_2\varphi_3^*)). \end{array} \right. \quad (10)$$

The $*$ represents the complex conjugate of a function and $G(|\varphi_2|^2)$ reads as [Gendelman, 2008; Lamarque *et al.*, 2011; Lamarque *et al.*, 2012]:

$$G(|\varphi_2|^2) = \begin{cases} 0 & \text{if } |\varphi_2| < \delta \\ \frac{1}{\pi} \left(2k \arccos\left(\frac{\delta}{|\varphi_2|}\right) - \frac{2\delta k \sqrt{|\varphi_2|^2 - \delta^2}}{|\varphi_2|^2} \right) & \text{if } |\varphi_2| \geq \delta. \end{cases} \quad (11)$$

Let us note that for the general Bouc–Wen model, we cannot obtain the general expression of the relation corresponding to the third equation of (10) which is obtained for the Dahl model. To deal with the introduced dynamical system, the multiple scales asymptotic approach [Nayfeh & Mook, 1979] by introducing slow times τ_1, τ_2, \dots with the fast time τ_0 will be implemented as follows:

$$T = \tau_0, \quad \tau_1 = \epsilon\tau_0, \quad \tau_2 = \epsilon^2\tau_0, \dots \quad (12)$$

so,

$$\frac{d}{dT} = \frac{\partial}{\partial\tau_0} + \epsilon \frac{\partial}{\partial\tau_1} + \epsilon^2 \frac{\partial}{\partial\tau_2} + \dots \quad (13)$$

In fact, instead of revealing the system behavior as a function of t directly, we embed it in a larger class of functions, determine a uniform expansion for each function as a function of time scales $\tau_0, \tau_1, \tau_2, \dots$, and then connect each function to the main system behavior at different transient and/or steady state regimes that are attracted according to the influence of the time scale. In the following sections, we will analyze the averaged system at different time scales in general and particularly with special attention to the system behaviors at the infinity of each time scale.

3. The Averaged System in ϵ^0 Order

Let us assume that $\frac{1-a}{a} = \epsilon a_0 = o(\epsilon)$. At the ϵ^0 order, system (10) yields:

$$\left\{ \begin{array}{l} \frac{\partial\varphi_1}{\partial\tau_0} = 0 \Rightarrow \varphi_1 = \varphi_1(\tau_1, \tau_2, \dots) \\ \frac{\partial\varphi_2}{\partial\tau_0} + \frac{i(1 - G(|\varphi_2|^2)) + \lambda}{2}\varphi_2 - \frac{i}{2}\varphi_1 = 0 \\ \varphi_3 = A\varphi_1 + \frac{i\beta e^{-i\delta_1}}{12\pi}(3\varphi_1\varphi_3 + e^{4i\delta_1}\varphi_1^*\varphi_3^* \\ \quad + 3e^{2i\delta_1}(\varphi_1^*\varphi_3 - \varphi_1\varphi_3^*)). \end{array} \right. \quad (14)$$

Fixed points $\Phi(\tau_0)$ of system (14) ($\tau_0 \rightarrow \infty$ and $\frac{\partial\varphi_2}{\partial\tau_0} \rightarrow 0$) are evaluated as:

$$\frac{i(1 - G(|\Phi|^2)) + \lambda}{2}\Phi = \frac{i}{2}\varphi_1. \quad (15)$$

If we consider that $\varphi_1 = N_1 e^{i\delta_1}$ and $\Phi = N_2 e^{i\delta_2}$, the following invariant manifold of the system and relationship between its phases at τ_0 time scale can be obtained:

$$N_1 = N_2 \sqrt{\lambda^2 + (1 - G(N_2^2))^2} \quad (16)$$

$$\delta_1 = \delta_2 - \arctan\left(\frac{\lambda}{1 - G(N_2^2)}\right). \quad (17)$$

It has been proved that the stable zone of the obtained invariant manifold of the system at τ_0 time scale, i.e. Eq. (16), is defined as [Lamarque *et al.*, 2011; Ture Savadkoochi *et al.*, 2012b]:

$$\lambda^2 + (1 - G(N_2^2))(1 - H(N_2^2)N_2 - G(N_2^2)) > 0 \quad (18)$$

where

$$H(N_2^2) = \begin{cases} 0, & N_2 < \delta \\ \frac{4\delta k}{\pi N_2^3} \sqrt{N_2^2 - \delta^2}, & N_2 \geq \delta. \end{cases} \quad (19)$$

The invariant manifold of a system with its stable borders are illustrated in Fig. 3. In fact, when the system reaches its unstable borders, it will try to jump to another stable border by a bifurcation. Forthcoming numerical results will validate this fact. Let us assume that $\varphi_3 = N_3 e^{i\delta_3}$. The third equation of the system (14) can be defined as:

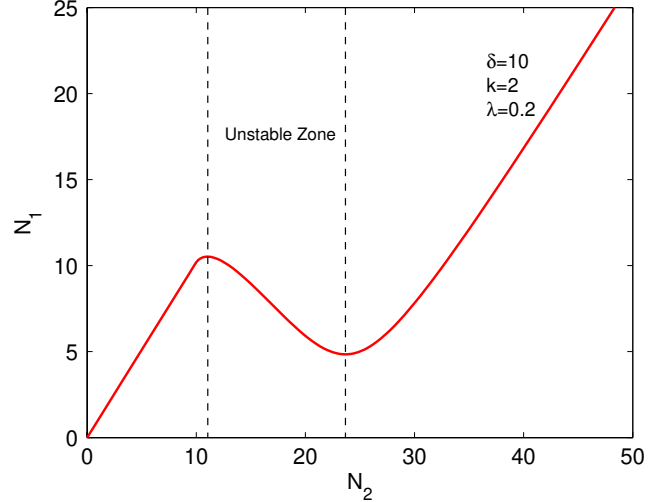


Fig. 3. Invariant manifold of a system at τ_0 time scale with unstable zone.

$$N_3 e^{i\delta_3} = AN_1 e^{i\delta_1} + \frac{i\beta}{12\pi} N_1 N_3 (6e^{i\delta_3} - 2e^{2i\delta_1} e^{-i\delta_3}). \quad (20)$$

After some mathematical treatments on Eq. (20) and the separation of the real and imaginary parts of the system, it can be proved that:

$$\begin{cases} \cos(\delta_3) = \frac{6AN_1\pi(6\pi \cos(\delta_1) + N_1\beta(-3 + \cos(2\delta_1)) \sin(\delta_1) + \cos(\delta_1) \sin(2\delta_1))}{N_3(36\pi^2 + 8N_1^2\beta^2)} \\ \sin(\delta_3) = \frac{-6AN_1\pi(-6\pi \sin(\delta_1) + N_1\beta((-3 + \cos(2\delta_1)) \cos(\delta_1) + \sin(\delta_1) \sin(2\delta_1))}{N_3(36\pi^2 + 8N_1^2\beta^2)}. \end{cases} \quad (21)$$

4. The Averaged System in ϵ^1 Order

The first equation of system (10) at the ϵ^1 order is defined as:

$$\begin{aligned} \frac{\partial \varphi_1}{\partial \tau_1} &= -\frac{i}{2} f_0 + \frac{i}{2} (-2\sigma - 1 + i\zeta) \varphi_1 \\ &+ \frac{i}{2} \varphi_2 + \frac{ia_0}{2} \varphi_3. \end{aligned} \quad (22)$$

We are interested to study the behavior of the system in τ_1 time scale “around” the state when τ_0 time scale has already reached infinity. This means that we always should take into account Eqs. (15)–(17) and (21) in all the forthcoming system of equations for detecting the system behavior at mentioned time layers. Equation (22) reads:

$$\frac{\partial}{\partial \tau_1} (\Phi - G(|\Phi|^2)\Phi - i\lambda\Phi)$$

$$\begin{aligned} &= -\frac{i}{2} f_0 + \frac{i}{2} (-2\sigma - 1 + i\zeta) \\ &\times (\Phi - G(|\Phi|^2)\Phi - i\lambda\Phi) \\ &+ \frac{i}{2} \Phi + \frac{ia_0}{2} \varphi_3. \end{aligned} \quad (23)$$

After some mathematical manipulations on Eq. (23), governing equations on the system at τ_1 time scale can be summarized as follows:

$$\begin{cases} \frac{\partial N_2}{\partial \tau_1} = \frac{(1 - G(N_2^2))\Xi - \lambda\Sigma}{g_1(N_2)} \\ \frac{\partial \delta_2}{\partial \tau_1} = \frac{1}{N_2} \frac{\lambda\Xi + (1 - G(N_2^2) - 2N_2^2 G'(N_2^2))\Sigma}{g_1(N_2)} \end{cases} \quad (24)$$

with

$$\Xi = -\frac{1}{2}f_0 \sin(\delta_2) - \frac{1}{2}N_2\lambda(2\sigma + 1) - \frac{1}{2}N_2\zeta(1 - G(N_2^2)) - \frac{1}{2}N_3a_0 \sin(\delta_3 - \delta_2) \quad (25)$$

$$\Sigma = -\frac{1}{2}f_0 \cos(\delta_2) - \frac{1}{2}N_2(1 - G(N_2^2))(2\sigma + 1) + \frac{1}{2}N_2\zeta\lambda + \frac{1}{2}N_2 + \frac{1}{2}N_3a_0 \cos(\delta_3 - \delta_2) \quad (26)$$

$$g_1(N_2) = (-1 + G(N_2^2))^2 + \lambda^2 + 2(-1 + G(N_2^2))N_2^2G'(N_2^2). \quad (27)$$

By considering Eq. (17) it can be proved that:

$$\begin{cases} N_3 \sin(\delta_3 - \delta_2) = \frac{\Upsilon_3(N_2)}{g_2(N_2)} \\ N_3 \cos(\delta_3 - \delta_2) = \frac{\Upsilon_4(N_2)}{g_2(N_2)} \end{cases} \quad (28)$$

$$\begin{cases} \Upsilon_3(N_2) = 3AN_2\pi(N_2\beta(-1 + G(N_2^2))(\lambda^2 + (-1 + G(N_2^2))^2) + 3\pi\lambda\sqrt{\lambda^2 + (-1 + G(N_2^2))^2}) \\ \Upsilon_4(N_2) = -3AN_2\pi(N_2\beta\lambda(\lambda^2 + (-1 + G(N_2^2))^2) - 3\pi(-1 + G(N_2^2))\sqrt{\lambda^2 + (-1 + G(N_2^2))^2}) \\ g_2(N_2) = \text{sign}(-1 + G(N_2^2))\sqrt{\lambda^2 + (-1 + G(N_2^2))^2} \times (9\pi^2 + 2N_2^2\beta^2(\lambda^2 + (-1 + G(N_2^2))^2)). \end{cases} \quad (29)$$

One can notice the influence of the Dahl model on system (24) due to the presence of A , β [in definitions of δ_3 in Eq. (21)] and a_0 .

4.1. Analysis of the system behavior at τ_1 time scale around invariants of τ_0 time scale

The system should be analyzed for clarifying possibilities of bifurcation(s) of the whole structure

during energy exchange between two oscillators. System (24) can be rewritten as:

$$\begin{cases} \frac{\partial N_2}{\partial \tau_1} = \frac{f_1(N_2, \delta_2)}{g_1(N_2)g_2(N_2)} \\ \frac{\partial \delta_2}{\partial \tau_1} = \frac{f_2(N_2, \delta_2)}{g_1(N_2)g_2(N_2)} \end{cases} \quad (30)$$

where $f_1(N_2, \delta_2)$ and $f_2(N_2, \delta_2)$ are numerators and $g(N_2) = g_1(N_2)g_2(N_2)$ is denominator of the governing equations of the system:

$$\begin{aligned} f_1(N_2, \delta_2) &= \left(g_2(N_2) \left(-\frac{1}{2}f_0 \sin(\delta_2) - \frac{1}{2}N_2\lambda(2\sigma + 1) - \frac{1}{2}N_2\zeta(1 - G(N_2^2)) \right) - \frac{a_0}{2}\Upsilon_3(N_2) \right) (1 - G(N_2^2)) \\ &+ \left(g_2(N_2) \left(-\frac{1}{2}f_0 \cos(\delta_2) - \frac{1}{2}N_2(1 - G(N_2^2))(2\sigma + 1) + \frac{1}{2}N_2\zeta\lambda + \frac{1}{2}N_2 \right) + \frac{a_0}{2}\Upsilon_4(N_2) \right) (-\lambda) \end{aligned} \quad (31)$$

$$\begin{aligned} N_2f_2(N_2, \delta_2) &= \left(g_2(N_2) \left(-\frac{1}{2}f_0 \sin(\delta_2) - \frac{1}{2}N_2\lambda(2\sigma + 1) - \frac{1}{2}N_2\zeta(1 - G(N_2^2)) \right) - \frac{a_0}{2}\Upsilon_3(N_2) \right) (\lambda) \\ &+ \left(g_2(N_2) \left(-\frac{1}{2}f_0 \cos(\delta_2) - \frac{1}{2}N_2(1 - G(N_2^2))(2\sigma + 1) + \frac{1}{2}N_2\zeta\lambda + \frac{1}{2}N_2 \right) + \frac{a_0}{2}\Upsilon_4(N_2) \right) \\ &\times (1 - G(N_2^2) - 2N_2^2G'(N_2^2)) \end{aligned} \quad (32)$$

Ordinary fixed points of the system are those who satisfy:

$$g(N_2, \delta_2) \neq 0, \quad \begin{cases} \frac{\partial N_2}{\partial \tau_1} = 0 \Rightarrow f_1(N_2, \delta_2) = 0 \\ \frac{\partial \delta_2}{\partial \tau_1} = 0 \Rightarrow f_2(N_2, \delta_2) = 0 \end{cases} \quad (33)$$

and fold singularities of the system are those who give:

$$g(N_2, \delta_2) = 0, \quad \begin{cases} \frac{\partial N_2}{\partial \tau_1} = 0 \Rightarrow f_1(N_2, \delta_2) = 0 \\ \frac{\partial \delta_2}{\partial \tau_1} = 0 \Rightarrow f_2(N_2, \delta_2) = 0. \end{cases} \quad (34)$$

In the latter case, the singularity and fixed points coincide. This case could lead us to very useful information about analyzing the flow of the system around its fold lines (i.e. $g(N_2, \delta_2) = 0$) in order to study SMR of the system [Starosvetsky & Gendelman, 2008; Lamarque *et al.*, 2011].

4.2. Stability analysis

We perturb the system as follows:

$$\begin{cases} N_2 \rightarrow N_2 + \Delta N_2 \\ \delta_2 \rightarrow \delta_2 + \Delta \delta_2 \end{cases} \quad (35)$$

By linearizing the equation of system (30) one can obtain the following equations:

$$\begin{bmatrix} \frac{\partial N_2}{\partial \tau_1} \\ \frac{\partial \delta_2}{\partial \tau_1} \end{bmatrix} = \Lambda \begin{bmatrix} \Delta N_2 \\ \Delta \delta_2 \end{bmatrix} \quad (36)$$

where

$$\Lambda = \frac{1}{g^2} \begin{bmatrix} \frac{\partial f_1}{\partial N_2} g - \frac{\partial g}{\partial N_2} f_1 & \frac{\partial f_1}{\partial \delta_2} g - \frac{\partial g}{\partial \delta_2} f_1 \\ \frac{\partial f_2}{\partial N_2} g - \frac{\partial g}{\partial N_2} f_2 & \frac{\partial f_2}{\partial \delta_2} g - \frac{\partial g}{\partial \delta_2} f_2 \end{bmatrix}. \quad (37)$$

Now, the linearized stability analysis can be carried out by looking at eigenvalues of the Λ matrix. As it was mentioned already at the exact position of fixed points $f_1 = f_2 = 0$, so Λ matrix can be simplified.

5. Some Examples

Here, some results are presented for three different external forcing terms.

5.1. $f_0 = 37$

All possible areas of the system with the external forcing term $f_0 = 37$ for given intervals where $f_1(N_2, \delta_2) = 0$ and $f_2(N_2, \delta_2) = 0$, are summarized in Fig. 4. Fold lines of the system which correspond to $g_1(N_2) = 0$ and $g_2(N_2) = 0$ (i.e. N_{21} , N_{22} and N_{23}) are illustrated in the same figure. In detail, N_{21} and N_{22} correspond to the solution of $g_1(N_2) = 0$, and are extremum points of the invariant manifold in τ_0 time scale [Lamarque *et al.*, 2011]. N_{23} corresponds to the solution of $g_2(N_2) = 0$. The intersections of $f_1(N_2, \delta_2) = 0$ and $f_2(N_2, \delta_2) = 0$ give positions of fixed points of the system at τ_1 time scales. The global view of the phase portrait of the system is depicted in Fig. 5. The behavior of the system around one fold fixed singularity (no. 3) and one normal fixed point (no. 5) in one period are illustrated in Figs. 6 and 7, respectively. A stability analysis can be carried out around these fixed points by examining eigenvalues of the matrix Λ in Eq. (37). It is seen from Fig. 6 that the fold singular point no. 3 is a saddle point which is unstable. The fixed point no. 5 is stable (from eigenvalues of Matrix Λ in Eq. (37) and Fig. 7).

The invariant manifold of a system with its stable borders which are obtained by Eqs. (16) and (18) are illustrated in Fig. 8. We also present

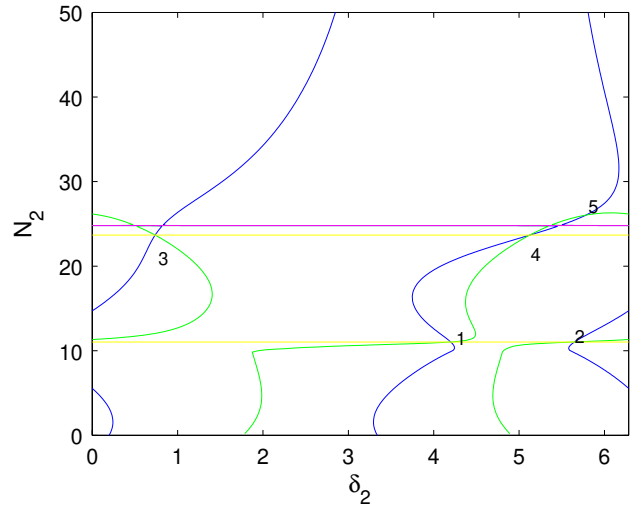


Fig. 4. $f_0 = 37$: $g_1(N_2) = 0$ (yellow), $g_2(N_2) = 0$ (magenta), $f_1(N_2, \delta_2) = 0$ (blue), $f_2(N_2, \delta_2) = 0$ (green). 1, 2, 3, 4: fold singularities, 5: stable fixed point.

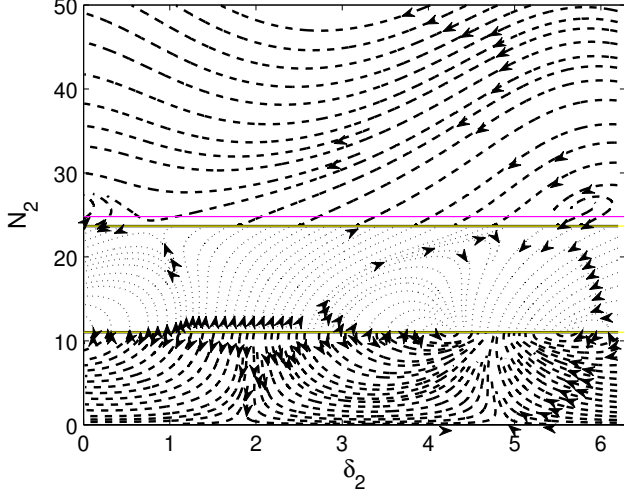


Fig. 5. General view of the phase portrait for the system with $f_0 = 37$.

results of direct integration of Eq. (3) by the “ode45” function of Matlab. Numerically obtained N_1 and N_2 which are mainly connected to the amplitudes of the main system and the NES, respectively (N_1^{num} and N_2^{num}) can be defined in terms of the original system of equations as follows:

$$N_1^{\text{num}} = \sqrt{(y_1 + \epsilon y_2)^2 + (\dot{y}_1 + \epsilon \dot{y}_2)^2} \quad (38)$$

$$N_2^{\text{num}} = \sqrt{(y_1 - y_2)^2 + (\dot{y}_1 - \dot{y}_2)^2}. \quad (39)$$

Moreover, we assume initial conditions which are given in (6). Added numerical results to analytical curve of Fig. 3 are depicted in Fig. 8. It can be seen that the averaged behavior of the system lies

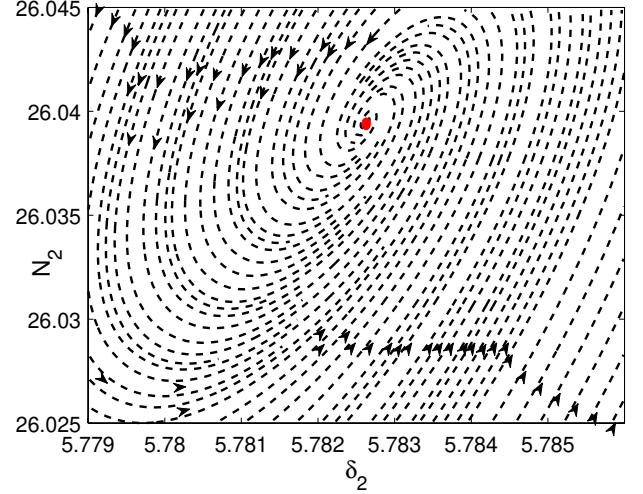


Fig. 7. Phase portrait of the system with $f_0 = 37$ around fixed point no. 5.

on the predicted averaged invariant manifold of the system. When the system reaches the stability border, it jumps to other stable branches via bifurcation. Looking at the variations of amplitudes of the main system (N_1) and the NES (N_2) with respect to time (see Fig. 9), the beating response or SMR of the overall system is evident. In fact after transient response of the system, variations of amplitudes of both oscillators become bounded by hysteresis bifurcations between stable branches of the overall system. Here, it can be seen that the bounded response of the main system presents small amplitude intervals for the main system and quite large

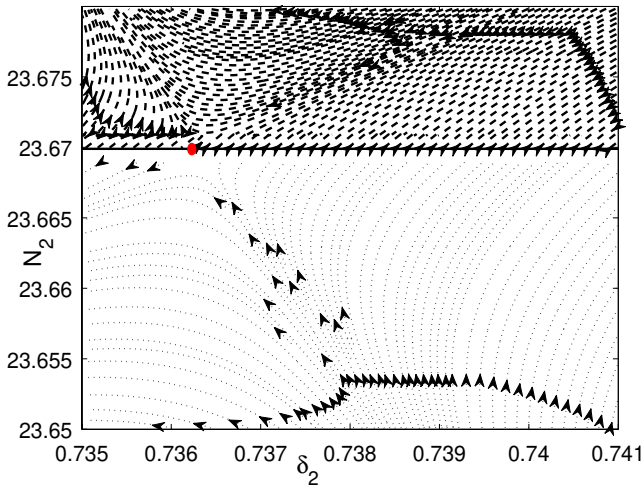


Fig. 6. Phase portrait of the system with $f_0 = 37$ around fixed point no. 3.

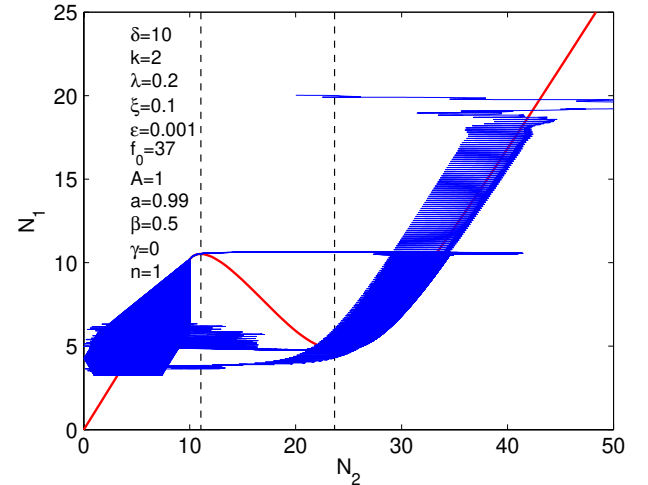
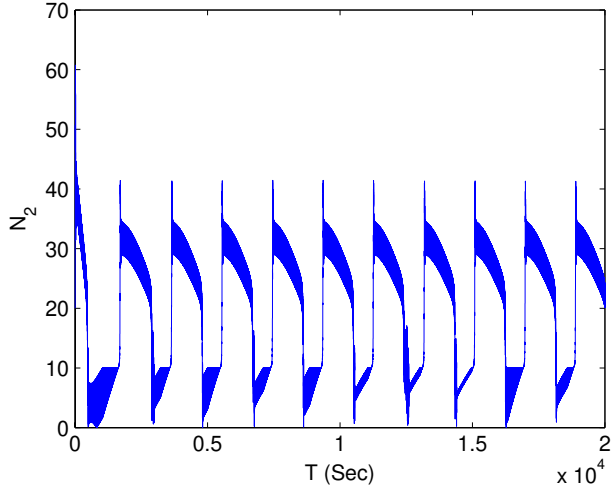
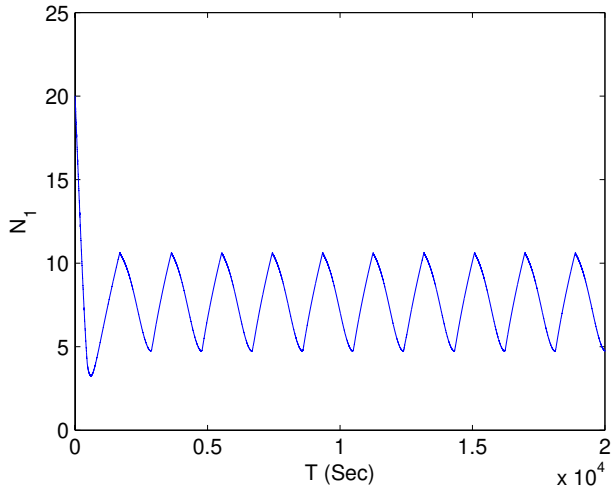


Fig. 8. Invariant manifold of a system at τ_0 time scale (red line), stability borders (dashed lines) and numerical results for $f_0 = 37$ (blue line). Starting points for numerical simulation are $(N_2, N_1) = (20, 20)$.



(a)



(b)

Fig. 9. Amplitude histories and beating responses of the system with $f_0 = 37$: (a) N_2 and (b) N_1 .

ones for the NES. This response shows that the NES is capable of controlling amplitudes of the main oscillator even if the NES finally presents bounded responses with quite large amplitudes. Explanations of this behavior for linear systems with coupled cubic/nonsmooth NES are given in [Starosvetsky & Gendelman, 2008; Lamarque *et al.*, 2011] where it is related to the existence of folded singularities on the fold line(s) of the system.

5.2. $f_0 = 50$

Here we examine the behavior of the system under a higher external forcing term. Zeros of the numerators and denominators of system (30) are depicted in Fig. 10 while its overall phase portrait is shown

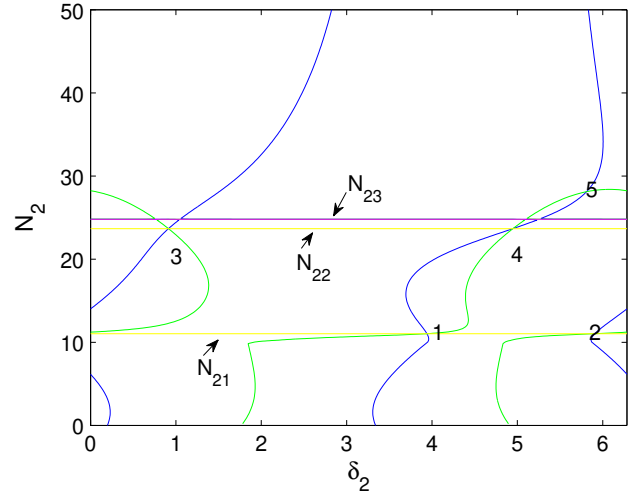


Fig. 10. $f_0 = 50$: $g_1(N_2) = 0$ (yellow), $g_2(N_2) = 0$ (magenta), $f_1(N_2, \delta_2) = 0$ (blue), $f_2(N_2, \delta_2) = 0$ (green). 1, 2, 3, 4: fold singularities, 5: stable fixed point.

in Fig. 11. The behavior of the system around fold singularity no. 4 (saddle and unstable) and normal fixed point no. 5 which is stable is depicted in Figs. 12 and 13, respectively. Added numerical results to the invariant manifold of the system and variations of N_1 and N_2 are collected in Figs. 14 and 15. Figure 15(a) shows that the averaged amplitudes of the NES after experiencing one SMR corresponds to the fixed point no. 5 in Fig. 10. In this case, final amplitudes of the main system [see Fig. 15(b)] may not be acceptable from the control point of view. It is worthwhile to mention that these interesting behaviors of the system and predictions

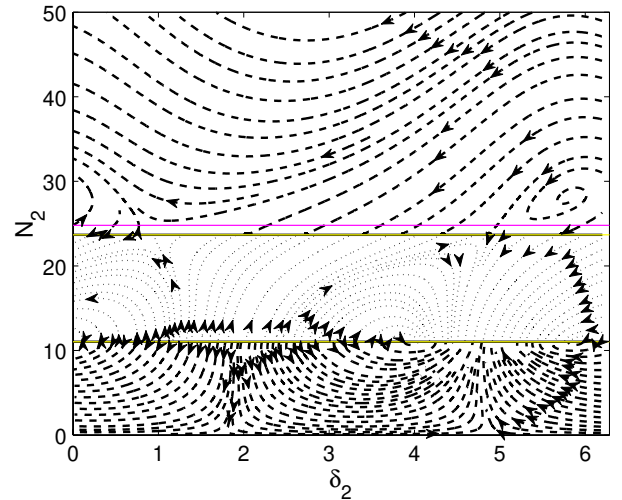


Fig. 11. General view of the phase portrait for the system with $f_0 = 50$.

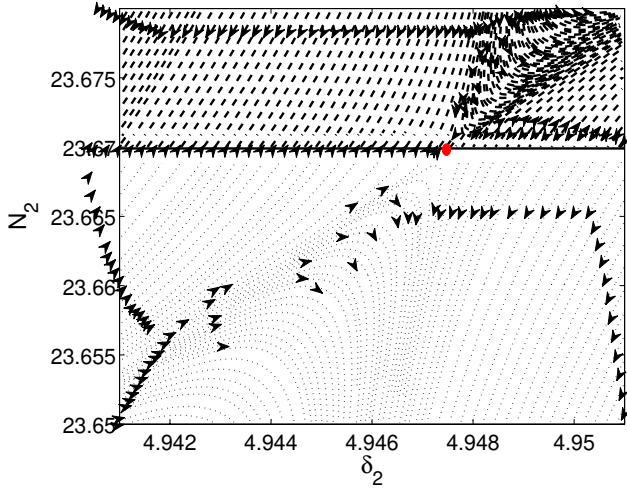


Fig. 12. Phase portrait of the system with $f_0 = 50$ around fixed point no. 4.

cannot be understood by studying only classical periodic steady-state solutions.

5.3. $f_0 = 100$

Let us consider the behavior of the system under $f_0 = 100$. The behavior of the system at τ_1 time scale is illustrated in Figs. 16 and 17 where added numerical results to the invariant manifold around τ_0 time scale are shown in Fig. 18, and the history of the system amplitudes are depicted in Fig. 19. Given results show that after one SMR, the system at the given time span, finally oscillates around fixed point no. 1 (see Fig. 20) that possesses very high amplitudes for both oscillators. This response

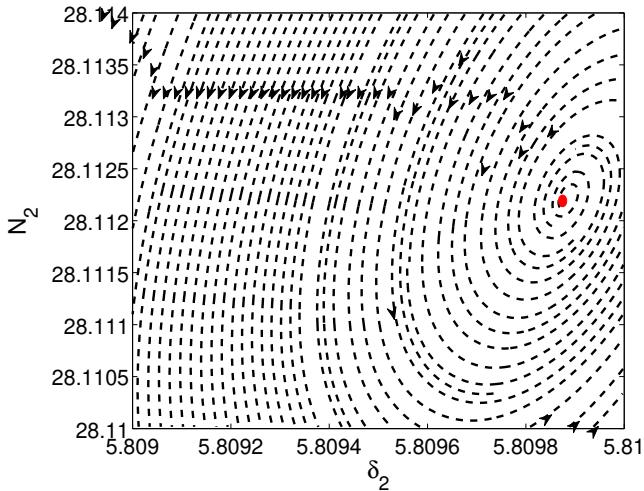


Fig. 13. Phase portrait of the system with $f_0 = 50$ around fixed point no. 5.

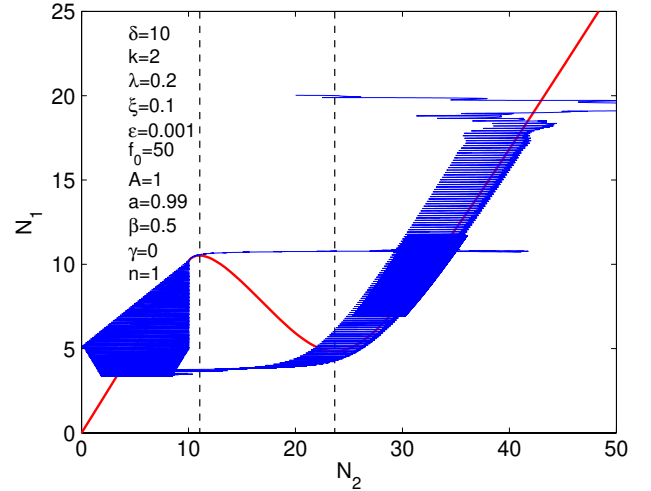


Fig. 14. Invariant manifold of a system at τ_0 time scale (red line), stability borders (dashed lines) and numerical results for $f_0 = 50$ (blue line). Starting points for numerical simulation are $(N_2, N_1) = (20, 20)$.

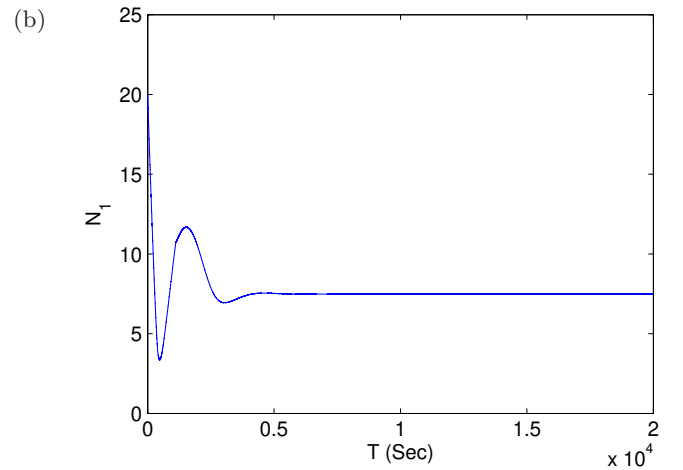
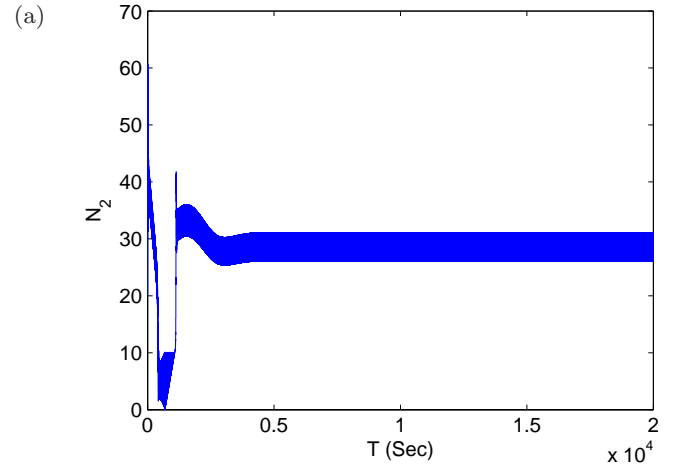


Fig. 15. Amplitude histories and beating responses of the system with $f_0 = 50$: (a) N_2 and (b) N_1 .

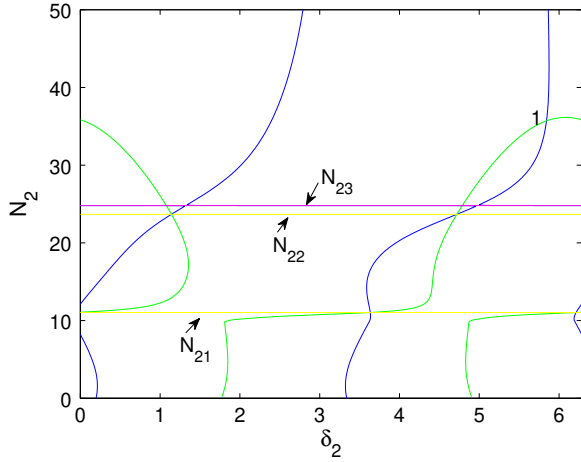
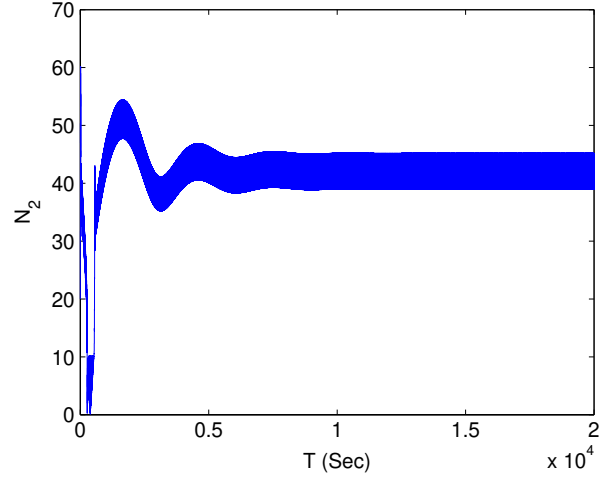


Fig. 16. $f_0 = 100$: $g_1(N_2) = 0$ (yellow), $g_2(N_2, \delta_2) = 0$ (magenta), $f_1(N_2, \delta_2) = 0$ (blue), $f_2(N_2, \delta_2) = 0$ (green).



(a)

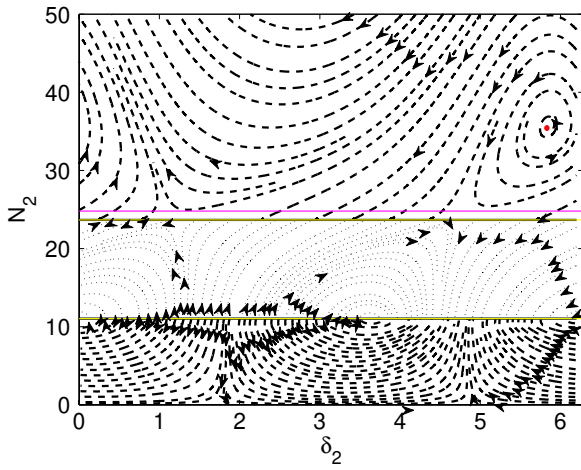
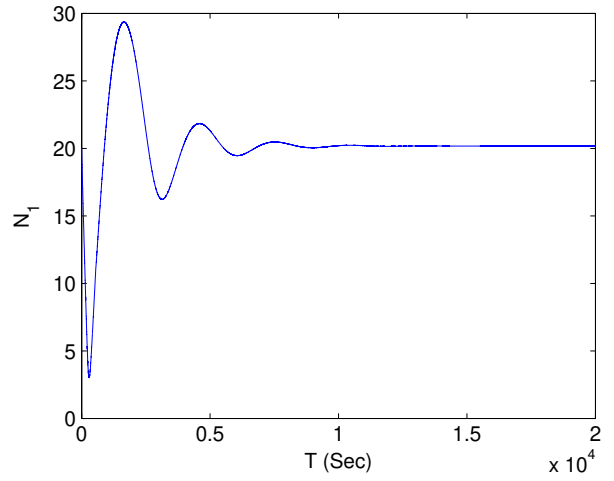


Fig. 17. General view of the phase portrait for the system with $f_0 = 100$.



(b)

Fig. 19. Amplitude histories of the system with $f_0 = 100$: (a) N_2 and (b) N_1 .

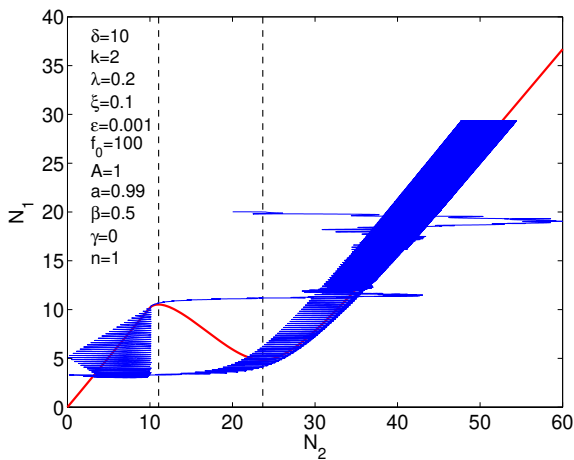


Fig. 18. Invariant manifold of a system at τ_0 time scale (red line), stability borders (dashed lines) and numerical results for $f_0 = 100$ (blue line). Starting points for numerical simulation are $(N_2, N_1) = (20, 20)$.

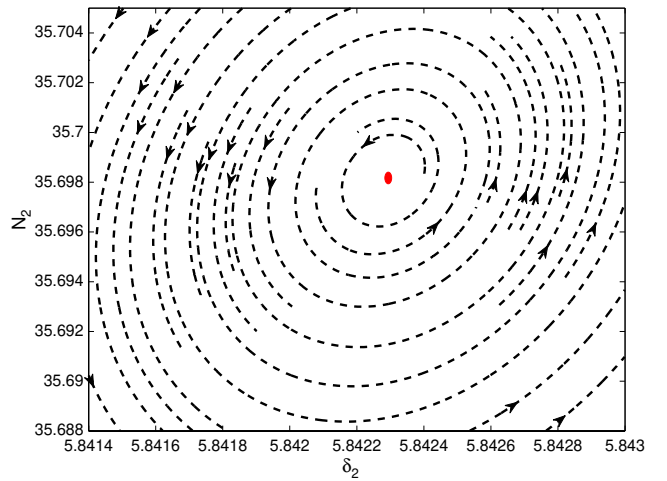


Fig. 20. Phase portrait of the system with $f_0 = 100$ around fixed point no. 1.

cannot be admitted from passive control view point and parameters of the NES should be changed.

6. Conclusions

The behavior of a system of two oscillators, a Dahl type oscillator and a coupled nonsmooth one, at two different time scales is studied. For practical investigations in industry, using nonsmooth energy sink is more realistic and more easy to be implemented — for instance, passive control process of systems in the presence of gravity where the symmetry can be destroyed due to the gravity [Ture Savadkoochi *et al.*, 2012b]. The multiscale developed technique lets us explain detailed behavior of the system while by classical methods it is impossible to do so. Detected dynamics of the system at the slow time scale traces all possible positions of pseudo-fixed points for understanding all possible attractions of the system at the same time scale around the invariant of the fast time scale. The system faces bifurcation(s) when it reaches the unstable zones of its invariant manifold at fast time scale and then depending on the existence of fold singularities at slow time scale, it may present reverse and hysteresis bifurcation(s). These developments are some steps toward the design of the light nonsmooth oscillator according to the focus of its usage. If the general goal is controlling the main system, the light nonsmooth oscillator should be tuned in such a way that the main system presents permissible (low) amplitude(s) interval(s) during the final periodic regime and/or its strongly modulated response. If the goal is harvesting the vibratory energy of the main system, then periodic and/or strongly modulated response with high energy levels and intervals for the main system can be permitted. The design process can be carried out by tuning parameters of coupled oscillator and analyzing system zeros and fold lines with their positions in Eq. (30). Future work will concern other Bouc–Wen models with more complicated expressions and also trying to analyze the effect of initial conditions of the response of the overall system by detecting “basin of attractions” of the system at different time scales.

References

- Awrejcewicz, J., Dzyubak, L. & Lamarque, C.-H. [2008] “Modelling of hysteresis using Masing–Bouc–Wen’s framework and search of conditions for the chaotic responses,” *Commun. Nonlin. Sci. Numer. Simul.* **13**, 939–958.
- Bouc, R. [1967] “Forced Vibration of Mechanical Systems with Hysteresis,” *Proceedings of the Fourth Conference on Nonlinear Oscillation* (Prague, Czechoslovakia).
- Bouc, R. [1971] “Modèle mathématique d’hystérésis,” *Acustica* **21**, 16–25.
- Casciati, F. [1987] “Nonlinear stochastic dynamics of large structural systems by equivalent linearization,” *Proc. 5th Int. Conf. Application of Statistics and Probability in Soil and Structural Engineering* (Vancouver, B.C., Canada).
- Dahl, P. R. [1968] *A Solid Friction Model* (The Aerospace Corporation, El-Segundo, TOR-158(3107-18), California).
- Gendelman, O. V., Manevitch, L. I., Vakakis, A. F. & M’Closkey, R. [2001] “Energy pumping in nonlinear mechanical oscillators I: Dynamics of the underlying Hamiltonian systems,” *ASME J. Appl. Mech.* **68**, 34–41.
- Gendelman, O. V. [2004] “Bifurcations of nonlinear normal modes of linear oscillator with strongly nonlinear damped attachment,” *Nonlin. Dyn.* **37**, 115–128.
- Gendelman, O. V. & Lamarque, C.-H. [2005] “Dynamics of linear oscillator coupled to strongly nonlinear attachment with multiple states of equilibrium,” *Chaos Solit. Fract.* **24**, 501–509.
- Gendelman, O. V., Gourdon, E. & Lamarque, C.-H. [2006] “Quasiperiodic energy pumping in coupled oscillators under periodic forcing,” *J. Sound Vibr.* **294**, 651–662.
- Gendelman, O. V. [2008] “Targeted energy transfer in systems with non-polynomial nonlinearity,” *J. Sound Vibr.* **315**, 732–745.
- Gendelman, O. V., Sapsis, T., Vakakis, A. F. & Bergman, L. A. [2011] “Enhanced passive targeted energy transfer in strongly nonlinear mechanical oscillators,” *J. Sound Vibr.* **330**, 1–8.
- Gourdon, E., Alexander, N. A., Taylor, C. A., Lamarque, C.-H. & Pernot, S. [2007a] “Nonlinear energy pumping under transient forcing with strongly nonlinear coupling: Theoretical and experimental results,” *J. Sound Vibr.* **300**, 522–551.
- Gourdon, E., Lamarque, C.-H. & Pernot, S. [2007b] “Contribution to efficiency of irreversible passive energy pumping with a strong nonlinear attachment,” *Nonlin. Dyn.* **50**, 793–808.
- Ikhoulane, F. & Rodellar, J. [2007] *Systems with Hysteresis* (John Wiley and Sons).
- Kerschen, G., Kowtko, J. J., McFarland, D. M., Bergman, L. A. & Vakakis, A. F. [2007a] “Theoretical and experimental study of multimodal targeted energy transfer in a system of coupled oscillators,” *Nonlin. Dyn.* **47**, 285–309.

- Kerschen, G., Kowtko, J. J., McFarland, D. M., Lee, Y. S., Bergman, L. A. & Vakakis, A. F. [2007b] “Experimental demonstration of transient resonance capture in a system of two coupled oscillators with essential stiffness nonlinearity,” *J. Sound Vibr.* **299**, 822–838.
- Lamarque, C.-H., Gendelman, O. V., Ture Savadkoohi, A. & Etcheverria, E. [2011] “Targeted energy transfer in mechanical systems by means of non-smooth nonlinear energy sink,” *Acta Mechanica* **221**, 175–200.
- Lamarque, C.-H., Ture Savadkoohi, A., Etcheverria, E. & Dimitrijevic, Z. [2012] “Multi-scales dynamics of two coupled nonsmooth systems,” *Int. J. Bifurcation and Chaos* **22**, 1250295–1–18.
- Lee, Y. S., Kerschen, G., McFarland, D. M., Hill, W. J., Nickkawde, C., Strganac, T. W., Bergman, L. A. & Vakakis, A. F. [2007] “Suppressing aeroelastic instability using broadband passive targeted energy transfers, part 2: Experiments,” *AIAA J.* **45**, 2391–2400.
- Lee, Y. S., Vakakis, A. F., Bergman, L. A., McFarland, D. M., Kerschen, G., Nucera, F., Tsakirtzis, S. & Panagopoulos, P. N. [2008] “Passive non-linear targeted energy transfer and its applications to vibration absorption: A review,” *Proc. Instit. Mech. Engin., Part K: J. Multi-Body Dynamics* **222**, 77–134.
- Lee, Y. S., Nucera, F., Vakakis, A. F., McFarland, D. M. & Bergman, L. A. [2009] “Periodic orbits, damped transitions and targeted energy transfers in oscillators with vibro-impact attachments,” *Physica D* **238**, 1868–1896.
- Lee, Y. S., Vakakis, A. F., McFarland, D. M. & Bergman, L. A. [2010] “Non-linear system identification of the dynamics of aeroelastic instability suppression based on targeted energy transfers,” *The Aeronautical J.* **114**, 61–82.
- Manevitch, L. I. [2001] “The description of localized normal modes in a chain of nonlinear coupled oscillators using complex variables,” *Nonlin. Dyn.* **25**, 95–109.
- Manevitch, L. I., Gourdon, E. & Lamarque, C.-H. [2007a] “Parameters optimization for energy pumping in strongly nonhomogeneous 2 dof system,” *Chaos Solit. Fract.* **31**, 900–911.
- Manevitch, L. I., Musienko, A. I. & Lamarque, C.-H. [2007b] “New analytical approach to energy pumping problem in strongly nonhomogeneous 2dof systems,” *Meccanica* **42**, 77–83.
- Manevitch, L. I., Gourdon, E. & Lamarque, C.-H. [2007c] “Towards the design of an optimal energetic sink in a strongly inhomogeneous two-degree-of-freedom system,” *Trans. ASME* **74**, 1078–1086.
- Manevitch, L. I., Kosevich, Y. A., Mane, M., Sigalov, G., Bergman, L. A. & Vakakis, A. F. [2011] “Towards a new type of energy trap: Classical analog of quantum Landau–Zener tunneling,” *Int. J. Non-Lin. Mech.* **46**, 247–252.
- McFarland, D. M., Bergman, L. & Vakakis, A. F. [2005a] “Experimental study of non-linear energy pumping occurring at a single fast frequency,” *Int. J. Non-Lin. Mech.* **40**, 891–899.
- McFarland, D. M., Kerschen, G., Kowtko, J. J., Lee, Y. S., Bergman, L. A. & Vakakis, A. F. [2005b] “Experimental investigation of targeted energy transfers in strongly and nonlinearly coupled oscillators,” *J. Acoust. Soc. America* **118**, 791–799.
- Nayfeh, A. H. & Mook, D. T. [1979] *Nonlinear Oscillations* (John Wiley and Sons, NY).
- Nucera, F., Vakakis, A. F., McFarland, D. M., Bergman, L. A. & Kerschen, G. [2007] “Targeted energy transfers in vibro-impact oscillators for seismic mitigation,” *Nonlin. Dyn.* **50**, 651–677.
- Pham, T. T., Pernot, S. & Lamarque, C.-H. [2010] “Competitive energy transfer between a two degree-of-freedom dynamic system and an absorber with essential nonlinearity,” *Nonlin. Dyn.* **62**, 573–592.
- Pham, T. T., Lamarque, C.-H. & Pernot, S. [2011a] “Passive control of one degree of freedom nonlinear quadratic oscillator under combination resonance,” *Commun. Nonlin. Sci. Numer. Simul.* **16**, 2279–2288.
- Pham, T. T., Lamarque, C.-H., Ture Savadkoohi, A. & Pernot, S. [2011b] “Multiple resonance capture of a compound system under harmonic excitation,” *European J. Comput. Mech.* **20**, 125–142.
- Pham, T. T., Lamarque, C.-H. & Ture Savadkoohi, A. [2012] “Multi-resonance capturing in a two-degree-of-freedom system under two different harmonic excitations,” *J. Vibr. Contr.* **18**, 451–466.
- Schmidt, F. & Lamarque, C.-H. [2010] “Energy pumping for mechanical systems involving non-smooth Saint-Venant terms,” *Int. J. Non-Lin. Mech.* **45**, 866–875.
- Song, J. & Der Kiureghian, A. [2006] “Generalized Bouc–Wen model for highly asymmetric hysteresis,” *J. Engin. Mech.* **132**, 610–618.
- Starosvetsky, Y. & Gendelman, O. V. [2008] “Strongly modulated response in forced 2DOF oscillatory system with essential mass and potential asymmetry,” *Physica D* **237**, 1719–1733.
- Starosvetsky, Y. & Gendelman, O. V. [2009] “Vibration absorption in systems with nonlinear energy sink: Nonlinear damping,” *J. Sound Vibr.* **324**, 916–939.
- Starosvetsky, Y. & Gendelman, O. V. [2010] “Interaction of nonlinear energy sink with a two degrees of freedom linear system: Internal resonance,” *J. Sound Vibr.* **329**, 1836–1852.
- Thyagarajan, R. S. & Iwan, W. D. [1990] “Performance characteristics of a widely used hysteretic model in structural dynamics,” *Proc. 4th U.S. National Conf. Earthquake Engineering* (Palm Springs, California).
- Ture Savadkoohi, A., Manevitch, L. I. & Lamarque, C.-H. [2011a] “Analysis of the transient behavior in

- a two dof nonlinear system,” *Chaos Solit. Fract.* **44**, 450–463.
- Ture Savadkoohi, A., Molinari, M., Bursi, O. S. & Friswell, M. I. [2011b] “Finite element model updating of a semi-rigid moment resisting structure,” *Struct. Contr. Health Monit.* **18**, 149–168.
- Ture Savadkoohi, A., Vaurigaud, B., Lamarque, C.-H. & Pernot, S. [2012a] “Targeted energy transfer with parallel nonlinear energy sinks, part II: Theory and experiments,” *Nonlin. Dyn.* **67**, 37–46.
- Ture Savadkoohi, A., Lamarque, C.-H. & Dimitrijevic, Z. [2012b] “Vibratory energy exchange between a linear and a non-smooth system in the presence of the gravity,” *Nonlin. Dyn.* **70**, 1473–1483.
- Vakakis, A. F. [2001] “Inducing passive nonlinear energy sinks in vibrating systems,” *ASME J. Vibr. Acoust.* **123**, 324–332.
- Vakakis, A. F. & Gendelman, O. V. [2001] “Energy pumping in nonlinear mechanical oscillators II: Resonance capture,” *ASME J. Appl. Mech.* **68**, 42–48.
- Vakakis, A. F., Gendelman, O. V., Bergman, L. A., McFarland, D. M., Kerschen, G. & Lee, Y. S. [2009a] *Nonlinear Targeted Energy Transfer in Mechanical and Structural Systems I* (Springer).
- Vakakis, A. F., Gendelman, O. V., Bergman, L. A., McFarland, D. M., Kerschen, G. & Lee, Y. S. [2009b] *Nonlinear Targeted Energy Transfer in Mechanical and Structural Systems II* (Springer).
- Vaurigaud, B., Manevitch, L. I. & Lamarque, C.-H. [2011a] “Passive control of aeroelastic instability in a long span bridge model prone to coupled flutter using targeted energy transfer,” *J. Sound Vibr.* **330**, 2580–2595.
- Vaurigaud, B., Ture Savadkoohi, A. & Lamarque, C.-H. [2011b] “Targeted energy transfer with parallel nonlinear energy sinks. Part I: Design theory and numerical results,” *Nonlin. Dyn.* **66**, 763–780.
- Vaurigaud, B., Ture Savadkoohi, A. & Lamarque, C.-H. [2011c] “Efficient targeted energy transfer with parallel nonlinear energy sinks: Theory and experiments,” *J. Comput. Nonlin. Dyn.* **6**, 041005-1–10.
- Viguié, R. & Kerschen, G. [2010] “On the functional form of a nonlinear vibration absorber,” *J. Sound Vibr.* **329**, 5225–5232.
- Wen, Y. K. [1976] “Method for random vibration of hysteretic systems,” *J. Engin. Mech. Div.* **102(EM2)**, 246–263.